Model for frequency-dependent nonlinear propagation in 2D-decorated nanowires

Nicolás Linale, Juan Bonetti, Alfredo D. Sánchez, Pablo I. Fierens, *Senior Member, IEEE*, and Diego F. Grosz

***Abstract*—We show that 2D-decorated silicon nanowires exhibit a strong frequency dependence of the real (Kerr) and imaginary (two-photon absorption) nonlinear coefficients. In this setting, we demonstrate that the usual extension of the nonlinear Schrödinger equation used to model propagation in this type of waveguides is rendered inadequate. Hence, we introduce a new modeling framework to tackle the frequency dependence of the nonlinear coefficients in 2D-decorated nanowires, and present an example of its application to the relevant case of supercontinuum generation in graphene- and graphene-oxide decorated silicon nanowires.**

***Index Terms*—Decorated nanowires, nonlinear optical pulse propagation**

I. Introduction

DECORATED nanowires have recently attracted the attention of researchers in nonlinear optics due to their large nonlinear coefficient [1]. As an example, graphene-decorated silicon nanowires, also referred to as graphene-on-silicon (GOS) nanowires, have been shown to exhibit a 10x increase of the nonlinear coefficient in the telecommunication band [2]–[4]. Furthermore, the compatibility with CMOS fabrication technologies [5], the wide transparency window of the silicon core in the mid-infrared range ($1.1 - 8.0$ μm) [6], and the large nonlinear coefficient altogether make GOS nanowires a compelling option for nonlinear integrated devices [1]. A relevant application of such devices is in the generation of supercontinuum (SC), oftentimes referred to as 'white light', a nonlinear process whereby a narrowband input pulse undergoes an extreme spectral broadening [7]. When such broad spectra are considered, the frequency dependence of the nonlinear Kerr coefficient, γ^{Kerr}, becomes of utmost importance. In particular, the effect of self-steepening (SS), related to the slope of the frequency dependence of γ^{Kerr} and responsible for the optical shock of ultrashort pulses [8] and the time-shift of optical solitons [9], among other manifestations, comes into play [10]–[12]. Further, two-photon absorption (TPA) is yet another nonlinear process of singular relevance in silicon nanowires [13], [14]. Although there are potential applications of TPA in the near- and mid-infrared [15]–[17], it usually represents a hindrance as it limits the spectral width of the generated supercontinuum [18]–[20]. The influence of TPA is usually modeled by introducing a complex-valued nonlinear coefficient $\gamma = \gamma^{\mathrm{Kerr}} + i\gamma^{\mathrm{TPA}}$ such that the imaginary part, $\gamma^{\mathrm{TPA}} = \beta^{\mathrm{TPA}}/2A_{\mathrm{eff}}$, accounts for two-photon absorption [15], [21], where β^{TPA} is the TPA coefficient and A_{eff} is the effective mode area of the nanowire.

It must be emphasized that even though several media exhibit strong frequency-dependent Kerr and TPA profiles [22], this dependence is oftentimes modeled by a simple linear relation $\gamma(\Omega) = \gamma_0(1 + s\Omega/\omega_0)$, where Ω is the deviation from a central frequency ω_0 and s is the SS parameter. Furthermore, s is customarily set to unity probably due to the fact that it is the only value which guarantees the conservation of the number of photons in the nonlinear Schrödinger equation (NLSE) [23]. In this work, however, we make apparent the inadequacy of assuming $s = 1$ in 2D-decorated nanowires, and thus a severe limitation of the NLSE when applied to the modeling of pulse propagation in this type of waveguides. For this reason, in Ref. [24] we introduced a new modeling equation, named the photon-conserving nonlinear Schrödinger equation (pc-NLSE) which, based on a quantum mechanical picture of the various nonlinear optical processes, guarantees strict conservation of the number of photons for any arbitrary frequency-dependent γ^{Kerr}. Moreover, the NLSE also exhibits problems when extended to include TPA by introducing a complex-valued nonlinear coefficient in straightforward fashion. Indeed, it can be shown that such an approach does not correctly model the cross-TPA of two co-propagating continuous waves (see Appendix B). This fact has led to the introduction of different modeling strategies. In particular, we extended the pc-NLSE to account for TPA in Ref. [25]. When modeling 2D-decorated nanowires, however, new challenges arise. While equations introduced in Refs. [24], [25] assume a homogeneous waveguide, decorated nanowires present very dissimilar optical properties in different regions of the cross section.

All in all, we come across three problems that need to be coped with when modeling nonlinear propagation

N. Linale, J. Bonetti, and D.F. Grosz are with the Depto. de Ingeniería en Telecomunicaciones, Centro Atómico Bariloche, GDTyPE, GAIyANN, Comisión Nacional de Energía Atómica (CNEA), Río Negro 8400, Argentina, and with Consejo Nacional de Investigaciones Científicas y Técnicas (CONICET), Argentina. Alfredo D. Sánchez was with CNEA and CONICET; he is currently at ICFO - Institut de Ciències Fotòniques, The Barcelona Institute of Science and Technology, 08860 Castelldefels (Barcelona), Spain

P. I. Fierens is with the Centro de Optoelectrónica, Instituto Tecnológico de Buenos Aires (ITBA), CABA 1106, Argentina, and with Consejo Nacional de Investigaciones Científicas y Técnicas (CONICET), Argentina.

in decorated nanowires. First, it is necessary to deal with media with disparate optical properties; second, the frequency dependence of the corresponding nonlinear coefficients has to be adequately accounted for; and third, two-photon absorption must be included into the model in a physical meaningful manner. In this paper we put forth an approach that addresses all these three problems, and present examples of its application to silicon nanowires decorated with thin layers of graphene and graphene oxide (GO).

The remaining of the work is organized as follows: In Section II we put forth a new modeling equation for decorated waveguides. In Section III we calculate the nonlinear coefficient for different decorating media of varying thickness. In Section IV we show an example of SC generation using the proposed model. Finally, Section V summarizes our conclusions.

II. Modeling Equation

Our starting point is an extension of the photon-conserving nonlinear Schrödinger equation [24]. The details of the derivation, although not overly difficult, are presented in Appendix A. The resulting modeling equation can be written as

$$\partial_z \tilde{A}_\Omega = -\frac{\alpha_{\text{eff}}}{2}\tilde{A}_\Omega + i\beta(\omega)\tilde{A}_\Omega + i\frac{\omega\zeta_!}{2}\mathcal{F}\left\{C_t\, B_t^2\right\} + i\frac{\omega\zeta_!}{2}\mathcal{F}\left\{B_t\, C_t^2\right\} - \omega\eta_!\,\mathcal{F}\left\{|D_t|^2 D_t\right\}, \tag{1}$$

where $\tilde{A}_\Omega = \tilde{A}(z,\Omega) = \mathcal{F}(A)$ is the Fourier transform of the complex envelope of the electric field $A_t = A(z,t)$, normalized so $|A|^2$ is the optical power, $\omega = \omega_0 + \Omega$ is the optical frequency of the Fourier component Ω, α_{eff} is the effective linear loss, and $\beta(\omega)$ is the dispersion profile. $\zeta_!$ and $\eta_!$ are related to the Kerr and TPA coefficients, respectively, through $\zeta_! = \sqrt[4]{\gamma_!^{\text{Kerr}}/\omega}$ and $\eta_! = \sqrt[4]{\gamma_!^{\text{TPA}}/\omega}$. The remaining fields, B_t, C_t, and D_t, are defined in the frequency domain by $\tilde{B}_\Omega = \zeta_!\,\tilde{A}_\Omega$, $\tilde{C}_\Omega = \zeta_!\,\tilde{A}_\Omega$, and $\tilde{D}_\Omega = \eta_!\,\tilde{A}_\Omega$. Finally, the nonlinear coefficient can be calculated as [26]

$$\gamma(\omega) = \frac{\omega}{c}\frac{\iint \overline{n}_2(x,y)|F(\omega,x,y)|^4\,dx\,dy}{\left(\iint |F(\omega,x,y)|^2\,dx\,dy\right)^2}, \tag{2}$$

where $F(\omega,x,y) \propto n(x,y)S(\omega,x,y)$, $n(x,y)$ is the linear refractive index, and $S(\omega,x,y)$ is the frequency-dependent mode distribution. We define the coefficient $\overline{n}_2$ as $\overline{n}_2 = n_2 + ic\beta^{\text{TPA}}/2\omega_0$ where n_2 and β^{TPA} are the nonlinear refractive index and the two-photon absorption coefficient, respectively. It must be noted that (1), which we shall also call pcNLSE, reduces to the usual NLSE whenever $\beta^{\text{TPA}} = 0$, $\gamma(\omega)$ is linear, and $s = 1$.

Observe that (1) does not include the effect of three-photon absorption (3PA), but it can be readily included by following the approach described in Appendix A. Likewise, the delayed Raman response can also be included into the pcNLSE as shown in Ref. [27]. Finally, the effects of free-carrier absorption (FCA), free-carrier dispersion (FCD), and saturable absorption can be neglected when dealing with ultrashort (femtosecond) pulses [20], [28], [29].

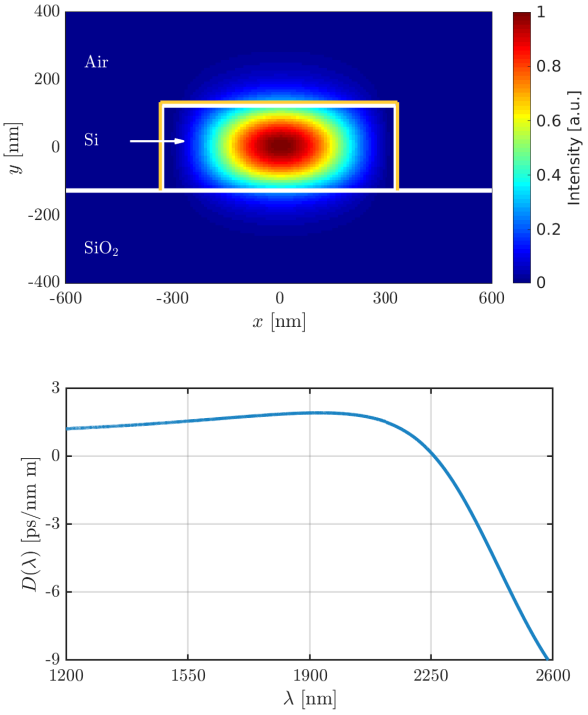

Fig. 1. Proposed waveguide: (Top) mode distribution and (bottom) dispersion $D(\ )$ of a silicon nanowire lying over a silicon-dioxide substrate. White lines separate different materials , and yellow lines indicate the 2D-decoration layer.

In what follows we will focus our attention on a 2D-decorated silicon nanowire. Since TPA in silicon is relevant up to ~ 2.2 μm [30] and three-photon absorption (3PA) becomes relevant from 2.2 to 3.3 μm [31], we will restrict our analysis to spectral content up to ~ 2.2 μm. Note also that Raman scattering can be neglected in silicon nanowires [20], [28], [32].

We modeled a 660-by-250 nm silicon nanowire lying over a silicon dioxide substrate and obtained the propagating transverse electric modes using the finite-difference time-domain (FDTD) algorithm [33]. Figure 1 (top) schematizes the waveguide and shows the mode distribution. Yellow lines represent the 2D-layer decoration surrounding the waveguide. The bottom panel in Fig. 1 shows the corresponding dispersion profile. We verified that this profile is essentially independent of the decorating material as long as its thickness, Λ, is considerable smaller than the transverse dimensions of the waveguide. This observation agrees with the very small fraction of mode overlap reported in the litera-

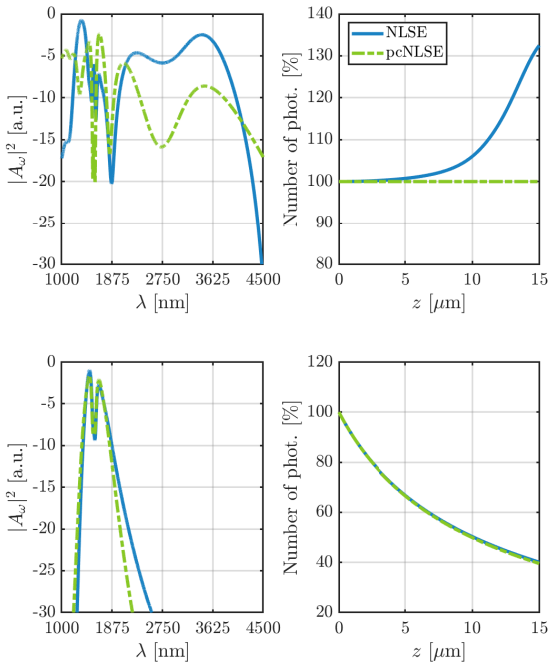

Fig. 2. Supercontinuum generation modeled with the NLSE (solid line) and with the pcNLSE (dashed-doted line), (top) neglecting and (bottom) including linear and nonlinear losses.

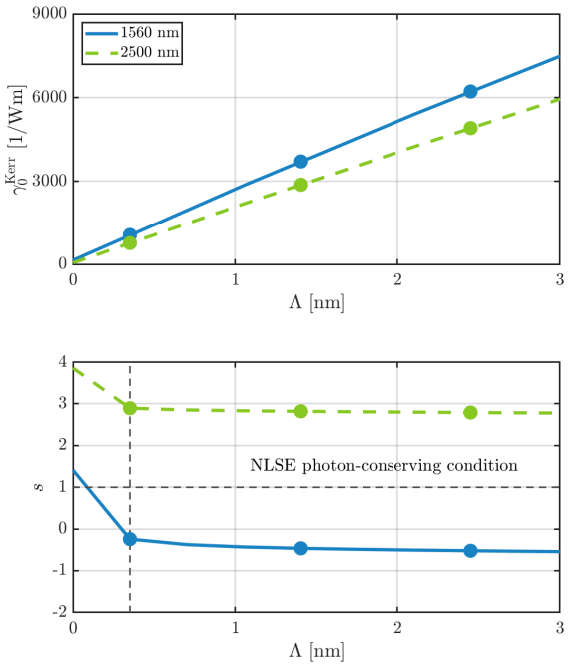

Fig. 3. (Top) Nonlinear coefficient and (bottom) SS parameter vs. thickness of the graphene-decorated nanowire, , at 1560 nm (solid line) and 2500 nm (dashed line). The vertical dashed line marks the thickness of a single graphene layer. Lines connecting data points are a guide to the eye.

ture [34]. Furthermore, the obtained dispersion profile agrees well with that in Ref. [4] where a silicon nanowire of similar dimensions was decorated with a single layer of graphene.

In order to fully comprehend the need for a complete modeling framework, in Fig. 2 we compare results of simulations of SC generation based on the nonlinear Schrödinger equation and the pcNLSE ((1)). Consistent with experimental parameters from Ref. [4], the input is a 438-W 20-fs half-width sech pulse at $\lambda_0 = 1560$ nm which propagates along a 15 μm-long GOS nanowire decorated with a graphene monolayer ($\Lambda \approx 0.35$ nm). The dispersion profile is that shown in the botton panel of Fig. 1. For the sake of clearness, results in Fig. 2 assume a linear dependence for the Kerr nonlinearity, $\gamma^{\mathrm{Kerr}}(\Omega) = \gamma_0^{\mathrm{Kerr}}(1+s\Omega/\omega_0)$, with $\gamma_0^{\mathrm{Kerr}} \approx 1150$ W ^{1}m ^{1}; the SS parameter is set to $s = -1$ in order to better reveal the differences between the two modeling equations. With the goal of properly studying the photon-number ($\propto \int_0^{R+1} |\tilde{A}|^2/(\hbar\omega)d\omega$) evolution, linear and nonlinear absorption are neglected in the top panel. Although proper modeling of propagation in decorated waveguides must include linear and nonlinear absorption, their effect conceals a basic shortcoming of the NLSE when applied to such systems, as made evident in the top panel of Fig. 2, where the evolution of the photon number is shown neglecting absorption effects. Observe that the NLSE predicts an unphysical increase in the number of photons while the pcNLSE strictly preserves it along propagation (top right panel). It is important to point out that this severe problem encountered when modeling with the NLSE is concealed when the effects of linear absorption, α, and TPA are considered. The bottom panel of Fig. 2 depicts this situation, where $\alpha = 0.052$ dB/μm [4] and $\gamma^{\mathrm{TPA}}(\Omega) = \gamma_0^{\mathrm{TPA}}(1 + s\Omega/\omega_0)$, with $\gamma_0^{\mathrm{TPA}} \approx 156$ W ^{1}m ^{1} and $s = -1$. Most interestingly, the two equations still predict different results for the output SC. Also, we observe that TPA severely limits the output spectral width [35], [36].

III. Calculation of the Nonlinear Parameter

Next, using (2) and the computed mode profile we calculated the Kerr nonlinearity and the self-steepening parameter as a function of the thickness of the decoration layer, and for relevant 2D-media such as graphene (Fig. 3) and graphene oxide (GO) (Fig. 4). The linear and nonlinear refractive indices, and linear and two-photon absorption coefficients for each medium are taken from the literature and presented in Appendix C. It is also

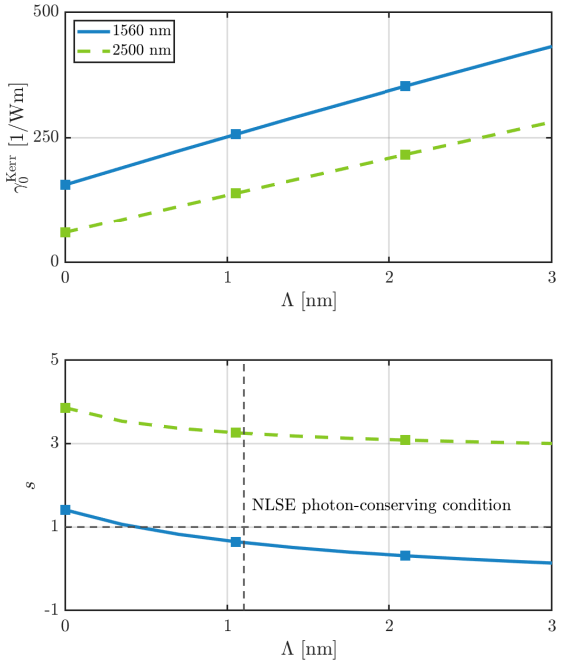

Fig. 4. (Top) Nonlinear coefficient and (bottom) SS parameter vs. thickness of the graphene-oxide-decorated nanowire, , at 1560 nm (solid line) and 2500 nm (dashed line). The vertical dashed line marks the thickness of a single graphene-oxide layer. Lines connecting data points are a guide to the eye.

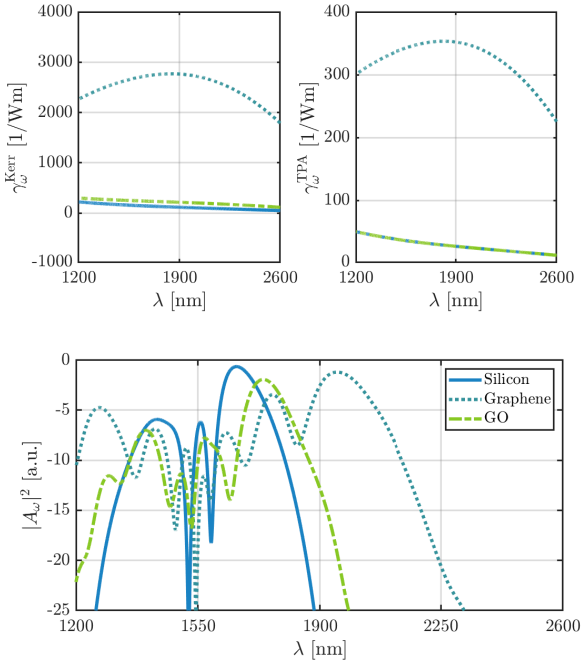

Fig. 5. Supercontinuum generation in nanowires. Top panels show the Kerr (left) and TPA (right) nonlinear coefficients vs. wavelength for a silicon nanowire (solid line), a graphene- (dashed line) and a graphene-oxide-decorated nanowire (dashed-dotted line).

important to point out that numerical integration of (2) requires a high resolution in the calculation of $F(\omega, x, y)$ in order to properly account for the thin decorating layer; however, such required resolution impairs the implementation of the FDTD algorithm. As a consequence, the mode is obtained with high resolution by means of a standard interpolation method of the low-resolution $F(\omega, x, y)$ calculated with the FDTD.

Results for the Kerr nonlinear coefficient and the SS parameter are shown in Figs. 3 (graphene) and 4 (GO), and for two different relevant wavelengths: one in the telecommunication band (1560 nm, solid-line) and the other in the mid IR (2500 nm, dashed-line). It is worth mentioning that the obtained nonlinear coefficient for graphene is in good agreement with that reported in Ref. [4]. Note that $\Lambda = 0$ corresponds to an undecorated waveguide and that the frequency dependence of the nonlinear coefficients comes from the mode effective area, A_{eff}, as both n_2 and β^{TPA} are assumed to be frequency independent. It can be observed that the Kerr coefficient increases with the decoration thickness for graphene and GO due to the increasing weight of these layers in the numerator of Eq. (2) [34]. This fact can be easily understood if, for the sake of argument, we neglect two-photon absorption and assume that the linear refractive index is constant and the same for both the waveguide and the 2D layer. Then, we can re-write Eq. (2) as

$$\gamma(\omega) = \frac{\omega}{cA_{\mathrm{eff}}} \left[\varepsilon n_2^{\mathrm{DL}} + (1-\varepsilon) n_2^{\mathrm{WG}} \right], \tag{3}$$

where n_2^{DL} and n_2^{WG} are the nonlinear refractive indices of the decorating layer and the waveguide, respectively, and

$$\varepsilon = \frac{\iint_{R_{\mathrm{DL}}} |S|^4 \, dxdy}{\iint |S|^4 \, dxdy}, \tag{4}$$

with R_{DL} the region corresponding to the decorating medium. As the number of layers increases, the region R_{DL} is enlarged and ε increases; as $n_2^{\mathrm{DL}} \gg n_2^{\mathrm{WG}}$ this results in an increase of $\gamma(\omega)$. If we now take into account the different refractive indices, a similar result still follows due to the fact that $n_2^{\mathrm{DL}}/n_2^{\mathrm{WG}} \gg n^{\mathrm{DL}}/n^{\mathrm{WG}}$, where n^{DL} and n^{WG} are the linear indices of the decorating layer and the waveguide, respectively. We must note that we have tacitly assumed that n_2^{DL} does not change as more layers are stacked. This fact has been observed to hold when considering a few layers (see, e.g., Refs. [37] and [38]).

The effective linear absorption of the decorated waveguide, α_{eff}, increases linearly with the number of decoration layers, a situation analogous to that of $\gamma(\omega)$.

The self-steepening parameter, on the contrary, remains nearly constant with Λ, a fact that might be related to the large weight of the zeroth-order nonlinear coefficient and the small thickness of the 2D decoration. It must be emphasized that large positive values of the self-steepening parameter are found for all three decorations in the mid IR, and even negative values of the SS parameter are found for graphene in the telecommunication band. Since all these values differ significantly from unity, the inadequacy of applying the NLSE to model optical pulse propagation in 2D-decorated nanowires becomes apparent. Indeed, observe that the NLSE-photon-conserving condition, $s = 1$, is only found in the undecorated waveguide and in the near infrared at 1560 nm.

Appendix D shows detailed guidelines for the application of the proposed method.

IV. Results

As an example of the application of the proposed modeling framework, let us focus on the supercontinuum generation in a silicon nanowire either undecorated or with a $\Lambda \approx 1.1$ nm decoration of graphene (~ 3 layers [39]) or graphene oxide (~ 1 layer [40]). The waveguide cross-section is that in Fig. 1 and its length is 150 μm. The frequency-dependent γ^{Kerr} and γ^{TPA}, computed according to (2) as in Figs. 3-4, are shown in the top panels of Fig. 5. Once again, the observed strong frequency dependence requires an adequate modeling equation such as (1). The bottom panel shows the output spectra when the input pulse is the same as that in Fig. 2. As it might be expected, the higher nonlinearity in the graphene-decorated waveguide leads to a much wider output spectrum as compared to the GO-decorated and the undecorated silicon waveguides. It is also interesting to observe that, even though the increase in the nonlinear Kerr coefficient is not as significant as in the case of graphene, the obtained output spectrum for the GO-decorated nanowire is still broader than that in the undecorated silicon nanowire. This is an important observation since TPA limits the attainable SC spectral width in long graphene-decorated nanowires, but TPA is substantially alleviated with the use of GO decoration, allowing for longer nanowires. We must note that the NLSE predicts wider spectra than those observed in Fig. 5.

V. Conclusions

In conclusion, we have introduced a new modeling framework that adequately deals with the frequency dependence of Kerr and TPA nonlinearities in decorated media, such as GOS nanowires, with an arbitrary thickness of the decoration layer. We have made apparent the need for such a modeling framework by explicitly calculating the mentioned wavelength-dependence in a typical silicon waveguide decorated with relevant 2D-media such as graphene and graphene oxide. Furthermore, we showed that usual extensions of the NLSE to model optical propagation in this type of waveguides are rendered inadequate as the self-steepening parameter can depart considerably from the NLSE photon-conserving condition. We believe that the model introduced in this work puts forth a powerful tool to model nonlinear propagation in cases of interest in applied integrated photonics.

	n_0	n_2 [m^2/W]	$^{\text{TPA}}$ [m/W]	References
Si	3.45	$4{:}2 \times 10^{-18}$	8×10^{-12}	[4]
SiO_2	1.45	3×10^{-20}	0	[8]
Graphene	3.65	10^{-13}	10^{-7}	[4]
GO	1.90	$1{:}38 \times 10^{-14}$	0	[34], [41]

TABLE I
Values of linear and nonlinear refractive indices, and two-photon absorption coefficients used in the simulations.

Appendix A
Inclusion of the TPA contribution into the propagation equation

We depart from a simple quantum theory for the propagation of optical pulses developed in Ref. [42]. Following an approach similar to that in Lai and Haus [43], it can be shown that the standard generalized nonlinear Schrödinger equation (for real $\gamma(\omega)$) can be derived from the quantum master equation

$$\frac{\partial \rho}{\partial z} = i \left[\hat{H}_{\text{Kerr}} + \hat{H}_{\text{R}}, \rho \right] \tag{5}$$

$$+ \int \hat{L}_{\text{R}}(\bar{\omega}) \rho \hat{L}_{\text{R}}^{\dagger}(\bar{\omega}) - \frac{1}{2} \left\{ \rho, \hat{L}_{\text{R}}^{\dagger}(\bar{\omega}) \hat{L}_{\text{R}}(\bar{\omega}) \right\} d\bar{\omega}, \tag{6}$$

where ρ is the density matrix representing the quantum state of the electromagnetic field, $\hat{H}_{\text{Kerr}}$ is the four-wave mixing operator associated with the Kerr effect, $\hat{H}_{\text{R}}$ is the four-wave mixing operator associated with the real part of the Raman response, and $\hat{L}_{\text{R}}(\bar{\omega})$ is the Lindbladian operator corresponding to the creation of a phonon of frequency $\bar{\omega}$. A detailed description of these operators is presented in Refs. [24], [27]. In particular, Ref. [27] shows that, in the classical limit, this approach leads to a photon-conserving generalized nonlinear Schrödinger equation (pcGNLSE) which ensures strict conservation of the photon number for any arbitrary frequency-dependent nonlinear profile, and which can be solved by the same tried and trusted numerical algorithms used for the standard generalized nonlinear Schrödinger equation. Note, however, that Eq. (1) in this work does not include the Raman contribution as it can be neglected in silicon nanowires.

In order to account for two-photon absorption (TPA), a new term must be added to the right-hand side of (6).

For the sake of clarity, let us focus only on this new term and write

$$\frac{\partial \rho}{\partial z} = \int \hat{L}_{\mathrm{TPA}}(\bar{\omega}) \rho \hat{L}^{\dagger}_{\mathrm{TPA}}(\bar{\omega}) \tag{7}$$

$$-\frac{1}{2} \left\{ \rho, \hat{L}^{\dagger}_{\mathrm{TPA}}(\bar{\omega}) \hat{L}_{\mathrm{TPA}}(\bar{\omega}) \right\} d\bar{\omega}, \tag{8}$$

where the Lindbladian operator $\hat{L}_{\mathrm{TPA}}(\bar{\omega})$ represents the two-photon absorption corresponding to an electron energy jump of $2\hbar\bar{\omega}$, and is defined as

$$\hat{L}_{\mathrm{TPA}}(\bar{\omega}) = \int \hat{\mathrm{D}}_{\nu+} \hat{\mathrm{D}}_{\nu} \, d\mu, \tag{9}$$

$$\hat{\mathrm{D}}_{\nu} = f_{\nu} \hat{A}_{\nu}. \tag{10}$$

$\hat{A}_{\nu}$ is a field operator related to the photon annihilation operator $\hat{a}_{\nu}$ by $\hat{A}_{\nu} = \sqrt{\hbar\omega}\hat{a}_{\nu}$ (see Ref. [42]), and f_{ν} is a function to be determined.

The mean value evolution of the field operator $\hat{A}_{\nu}$ is given by

$$\frac{\partial \langle \hat{A}_{\nu} \rangle}{\partial z} = \frac{1}{2} \int \left[\hat{L}^{\dagger}_{\mathrm{TPA}}(\bar{\omega}), \hat{A}_{\nu} \right] \hat{L}_{\mathrm{TPA}}(\bar{\omega}) \tag{11}$$

$$-\hat{L}^{\dagger}_{\mathrm{TPA}}(\bar{\omega}) \left[\hat{A}_{\nu}, \hat{L}_{\mathrm{TPA}}(\bar{\omega}) \right] d\bar{\omega}. \tag{12}$$

Substitution of (9) into (12) leads to

$$\frac{\partial \langle \hat{A}_{\nu} \rangle}{\partial z} = -\hbar\omega f_{\nu} \int\int \langle \hat{\mathrm{D}}^{\dagger}_{2\tau} \, {}_{\nu}\hat{\mathrm{D}}_{\tau+} \, \hat{\mathrm{D}}_{\tau} \rangle \, d\mu \, d\bar{\omega}$$

$$= -\hbar\omega \int\int f_{\nu} f_{2\tau} \, {}_{\nu}f_{\tau+} \, f_{\tau} \langle \hat{A}^{\dagger}_{2\tau} \, {}_{\nu}\hat{A}_{\tau+} \, \hat{A}_{\tau} \rangle \, d\mu \, d\bar{\omega}, \tag{13}$$

where we used the fact that $[\hat{a}_{\nu}, \hat{a}^{\dagger}_{\nu'}] = \delta(\omega - \omega^{0})$. In the classical limit, this last equation reads

$$\frac{\partial \tilde{A}_{\nu}}{\partial z} = -\hbar\omega f_{\nu} \int\int \tilde{\mathrm{D}}_{2\tau} \, {}_{\nu}\tilde{\mathrm{D}}_{\tau+} \, \tilde{\mathrm{D}}_{\tau} \, d\mu \, d\bar{\omega}$$

$$= -\hbar\omega \int\int f_{\nu} f_{2\tau} \, {}_{\nu}f_{\tau+} \, f_{\tau} \, \tilde{A}_{2\tau} \, {}_{\nu}\tilde{A}_{\tau+} \, \tilde{A}_{\tau} \, d\mu \, d\bar{\omega}, \tag{14}$$

with $\tilde{\mathrm{D}}_{\nu} = f_{\nu} \tilde{A}_{\nu}$.

In order to determine f_{ν}, let us focus on the simple case of a continuous wave (CW)

$$\tilde{A}_{\nu}(z) = 2\pi\delta(\omega - \omega_0) \sqrt{P_0(z)}, \tag{15}$$

where P_0 is the optical power and ω_0 is the CW frequency. By introducing (15) in (14), we find that the evolution of the optical power is described by

$$\frac{\partial P_0}{\partial z} = -8\pi^2 \hbar\omega_0 |f_{\nu 0}|^2 P_0^2. \tag{16}$$

The intensity of the CW can be calculated as $I_0 = P_0/A_{\mathrm{eff}}(\omega_0)$, where A_{eff} is the effective area of the waveguide (see, e.g., Chapter 2 in Ref. [8]). The evolution of the intensity is thus given by

$$\frac{\partial I_0}{\partial z} = -8\pi^2 \hbar\omega_0 A_{\mathrm{eff}}(\omega_0) |f_{\nu 0}|^2 I_0^2. \tag{17}$$

This equation must agree with the basic phenomenological description of TPA based on the effective loss coefficient, $\beta^{\mathrm{TPA}}_{\mathrm{eff}} = 2\gamma^{\mathrm{TPA}}_{\nu} A_{\mathrm{eff}}(\omega)$, and the equation

$$\frac{\partial I_0}{\partial z} = -\beta^{\mathrm{TPA}}_{\mathrm{eff}} I_0^2. \tag{18}$$

Comparison of (17) and (18) leads to

$$f_{\nu} = \sqrt{\frac{\beta^{\mathrm{TPA}}_{\mathrm{eff}}}{8\pi^2 \hbar\omega A_{\mathrm{eff}}(\omega)}}. \tag{19}$$

For the sake of notation clarity, let us introduce $\eta_{\nu} = \sqrt{\gamma^{\mathrm{TPA}}_{\nu}/\omega}$. By replacing (19) in (14), we obtain

$$\frac{\partial \tilde{A}_{\nu}}{\partial z} = -\omega\eta_{\nu} \mathcal{F} \left\{ |D_t|^2 D_t \right\}, \tag{20}$$

where $D_t = \mathcal{F}^{-1}[\tilde{D}_{\nu}]$ and $D_{\nu} = \eta_{\nu} \tilde{A}_{\nu}$. Finally, the right-hand side of Eq. (20) is the TPA contribution added to the pcNLSE in Eq. (1).

A comment is due on the relation of this modeling framework to our previous work in Ref. [25]. Indeed, the definition of the Linbladian operator in (9), describing the TPA process in terms of photon annihilation operators is similar to an analogous one in Ref. [25]. However, in the context of 2D-decorated nanowires we assumed that, for the spectral region of interest, $\beta^{\mathrm{TPA}}_{\mathrm{eff}}$ is essentially independent of the wavelength and changes in $\gamma^{\mathrm{TPA}}_{\nu}$ are introduced by the frequency-dependence of the transverse mode distribution. This assumption leads to a simpler propagation equation than that introduced in our earlier work. Furthermore, in this paper we account for the disparities in the nonlinear coefficients of the different materials in the waveguide.

APPENDIX B
CROSS-TPA OF TWO CONTINUOUS WAVES

Propagation in nonlinear waveguides is usually modeled with the standard nonlinear Schrödinger equation (NLSE) [8],

$$\frac{\partial \tilde{A}_{\Omega}}{\partial z} = i\beta(\omega)\tilde{A}_{\Omega} + i\gamma(\omega) \mathcal{F} \left\{ |A_t|^2 A_t \right\}, \tag{21}$$

which describes the evolution of the normalized complex envelope of the electric field $A_t = A(z,t)$, and where $\tilde{A}_{\Omega} = \tilde{A}(z,\Omega) = \mathcal{F}(A)$ is its Fourier transform, $|A|^2$ the optical power, $\omega = \omega_0 + \Omega$ the optical frequency of the Fourier component Ω, ω_0 the envelope central frequency, and $\beta(\omega)$ and $\gamma(\omega)$ are the dispersion and nonlinear profiles, respectively. It is straightforward to show that, under the NLSE, the evolution of photon fluxes of two co-propagating continuous waves of frequencies ω_1 and ω_2 is given

$$\begin{aligned} \partial_z \Phi_1 &= -\hbar\omega_1 \gamma^{\mathrm{TPA}}_{\nu_1} \Phi_1^2 - 2\hbar\omega_2 \gamma^{\mathrm{TPA}}_{\nu_1} \Phi_1 \Phi_2 \\ \partial_z \Phi_2 &= -\hbar\omega_2 \gamma^{\mathrm{TPA}}_{\nu_2} \Phi_2^2 - 2\hbar\omega_1 \gamma^{\mathrm{TPA}}_{\nu_2} \Phi_1 \Phi_2, \end{aligned} \tag{22}$$

where $\Phi_j = |\tilde{A}(\omega_j)|^2/\hbar\omega_j$. Note that (22) is obtained by neglecting all other frequencies resulting from four-wave mixing interactions between ω_1 and ω_2. Note also

that this evolution is not in agreement with the expected behavior of a TPA process, as the cross-terms containing $\Phi_1\Phi_2$ should be identical in order to correctly account for photon absorption due to the cross-TPA between the two CWs.

A similar analysis departing from (20) leads to

$$\begin{aligned}\partial_z\Phi_1 &= -\hbar\omega_1\gamma_{I_1}^{\mathrm{TPA}}\Phi_1^2 - 2\kappa^{\mathrm{XTPA}}\Phi_1\Phi_2 \\ \partial_z\Phi_2 &= -\hbar\omega_2\gamma_{I_2}^{\mathrm{TPA}}\Phi_2^2 - 2\kappa^{\mathrm{XTPA}}\Phi_1\Phi_2,\end{aligned} \tag{23}$$

where $\kappa^{\mathrm{XTPA}} = \hbar \sqrt{\omega_1\gamma_{I_1}^{\mathrm{TPA}}\omega_2\gamma_{I_2}^{\mathrm{TPA}}}$. Unlike (22), cross-TPA terms in (23) are identical, as expected, providing support to the physical validity of our approach.

APPENDIX C
SIMULATION PARAMETERS

The effective linear absorption coefficients used the in simulations are $\alpha_{\mathrm{eff}} = 1.19 \times 10^4$ [4], 1.19×10^2 [34], [41], and $0.8\ \mathrm{m}^{-1}$ [44] for graphene, graphene oxide, and silicon, respectively. The linear and nonlinear refractive indices, and the two-photon absorption coefficients are summarized in Table I. Note that it is customary to define an equivalent nonlinear refractive index for a single layer of graphene [38], [39]. Moreover, since the third-order susceptibility of stacked layers of graphene has been shown to scale linearly with the number of layers, n_2 can be considered to be roughly independent of the thickness of the 2D-decoration [45], an assumption we also make when modeling the graphene-oxide decoration.

APPENDIX D
GUIDELINES FOR THE APPLICATION OF THE PROPOSED METHOD

In Section II, we model propagation in 2D-decorated waveguides following three steps:

1) The quasi-TE modes of the waveguide are computed by using a Finite-Difference Time-Domain (FDTD) algorithm. The 2D decorating layer does not need to be taken into account in this step.
2) $\gamma(\omega)$ is calculated by means of Eq. (2), thus properly accounting for the influence of the 2D layer on the nonlinear coefficient.
3) Eq. (1) is used to model propagation in the decorated waveguide. This equation can be solved by widely tried and trusted numerical algorithms such as the split-step Fourier [46].

REFERENCES

[1] S. Yamashita, "Nonlinear optics in carbon nanotube, graphene, and related 2d materials," *APL Photonics*, vol. 4, no. 3, p. 034301, 2019.

[2] Z. Zhang and P. L. Voss, "Full-band quantum-dynamical theory of saturation and four-wave mixing in graphene," *Optics Letters*, vol. 36, no. 23, pp. 4569–4571, 2011.

[3] N. Vermeulen, D. Castelló-Lurbe, J. Cheng, I. Pasternak, A. Krajewska, T. Ciuk, W. Strupinski, H. Thienpont, and J. Van Erps, "Negative kerr nonlinearity of graphene as seen via chirped-pulse-pumped self-phase modulation," *Physical Review Applied*, vol. 6, no. 4, p. 044006, 2016.

[4] A. Ishizawa, R. Kou, T. Goto, T. Tsuchizawa, N. Matsuda, K. Hitachi, T. Nishikawa, K. Yamada, T. Sogawa, and H. Gotoh, "Optical nonlinearity enhancement with graphene-decorated silicon waveguides," *Scientific Reports*, vol. 7, p. 45520, 2017.

[5] B. Kuyken, T. Ideguchi, S. Holzner, M. Yan, T. W. Hänsch, J. Van Campenhout, P. Verheyen, S. Coen, F. Leo, R. Baets *et al.*, "An octave-spanning mid-infrared frequency comb generated in a silicon nanophotonic wire waveguide," *Nature Communications*, vol. 6, no. 1, pp. 1–6, 2015.

[6] R. Soref, "Mid-infrared photonics in silicon and germanium," *Nature Photonics*, vol. 4, no. 8, pp. 495–497, 2010.

[7] J. M. Dudley, G. Genty, and S. Coen, "Supercontinuum generation in photonic crystal fiber," *Reviews of Modern Physics*, vol. 78, no. 4, p. 1135, 2006.

[8] G. P. Agrawal, *Nonlinear Fiber Optics*. Academic Press, 2013.

[9] N. Linale, P. I. Fierens, J. Bonetti, A. D. Sánchez, S. M. Hernandez, and D. F. Grosz, "Measuring self-steepening with the photon-conserving nonlinear Schrödinger equation," *Optics Letters*, vol. 45, no. 16, pp. 4535–4538, 2020.

[10] B. Kibler, J. Dudley, and S. Coen, "Supercontinuum generation and nonlinear pulse propagation in photonic crystal fiber: influence of the frequency-dependent effective mode area," *Applied Physics B*, vol. 81, no. 2-3, pp. 337–342, 2005.

[11] L. Zhang, Y. Yan, Y. Yue, Q. Lin, O. Painter, R. G. Beausoleil, and A. E. Willner, "On-chip two-octave supercontinuum generation by enhancing self-steepening of optical pulses," *Optics Express*, vol. 19, no. 12, pp. 11 584–11 590, 2011.

[12] M. A. Gaafar, T. Baba, M. Eich, and A. Y. Petrov, "Front-induced transitions," *Nature Photonics*, vol. 13, no. 11, pp. 737–748, 2019.

[13] D. Hutchings and E. W. Van Stryland, "Nondegenerate two-photon absorption in zinc blende semiconductors," *Journal of the Optical Society of America B*, vol. 9, no. 11, pp. 2065–2074, 1992.

[14] Y.-R. Shen, *The principles of nonlinear optics*. Wiley-Interscience, 1984.

[15] Q. Lin, O. J. Painter, and G. P. Agrawal, "Nonlinear optical phenomena in silicon waveguides: modeling and applications," *Optics Express*, vol. 15, no. 25, pp. 16 604–16 644, 2007.

[16] X. Liu, R. M. Osgood Jr, Y. A. Vlasov, and W. M. Green, "Mid-infrared optical parametric amplifier using silicon nanophotonic waveguides," *Nature Photonics*, vol. 4, no. 8, p. 557, 2010.

[17] N. Poulvellarie, C. Ciret, B. Kuyken, F. Leo, and S.-P. Gorza, "Highly nondegenerate two-photon absorption in silicon wire waveguides," *Physical Review Applied*, vol. 10, no. 2, p. 024033, 2018.

[18] P. Koonath, D. R. Solli, and B. Jalali, "Limiting nature of continuum generation in silicon," *Applied Physics Letters*, vol. 93, no. 9, p. 091114, 2008.

[19] I.-W. Hsieh, X. Chen, J. I. Dadap, N. C. Panoiu, R. M. Osgood, S. J. McNab, and Y. A. Vlasov, "Ultrafast-pulse self-phase modulation and third-order dispersion in si photonic wire-waveguides," *Optics Express*, vol. 14, no. 25, pp. 12 380–12 387, 2006.

[20] L. Yin, Q. Lin, and G. P. Agrawal, "Soliton fission and supercontinuum generation in silicon waveguides," *Optics Letters*, vol. 32, no. 4, pp. 391–393, 2007.

[21] P. Paufler, "Pn butcher, d. cotter the elements of nonlinear optics. cambridge university press. cambridge 1990, xiv+ 344p. preis£ 30.00, isbn 0-521-34183-3," *Crystal Research and Technology*, vol. 26, no. 6, pp. 802–802, 1991.

[22] N. C. Panoiu, X. Liu, and R. M. Osgood Jr, "Self-steepening of ultrashort pulses in silicon photonic nanowires," *Optics Letters*, vol. 34, no. 7, pp. 947–949, 2009.

[23] K. Blow and D. Wood, "Theoretical description of transient stimulated Raman scattering in optical fibers," *IEEE Journal of Quantum Electronics*, vol. 25, no. 12, pp. 2665–2673, Dec. 1989.

[24] J. Bonetti, N. Linale, A. D. Sánchez, S. M. Hernandez, P. I. Fierens, and D. F. Grosz, "Modified nonlinear Schrödinger equation for frequency-dependent nonlinear profiles of arbitrary sign," *Journal of the Optical Society of America B*, vol. 36, no. 11, pp. 3139–3144, 2019.

[25] N. Linale, J. Bonetti, A. Sparapani, A. D. Sánchez, and D. F. Grosz, "Equation for modeling two-photon absorption in nonlinear waveguides," *Journal of the Optical Society of America B*, vol. 37, no. 6, pp. 1906–1910, 2020.

[26] Y. Yang, J. Wu, X. Xu, Y. Liang, S. T. Chu, B. E. Little, R. Morandotti, B. Jia, and D. J. Moss, "Invited article: Enhanced four-wave mixing in waveguides integrated with graphene oxide," *APL Photonics*, vol. 3, no. 12, p. 120803, 2018.